Energy Conversion and Management 293 (2023) 117546

Contents lists available at ScienceDirect

Energy Conversion and Management

journal homepage: www.elsevier.com/locate/enconman

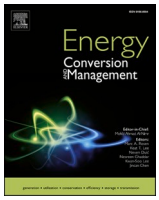

Thermodynamic study of organic Rankine cycle based on extraction steam compression regeneration in the supercritical state

Enhui Sun [a,b,*], Yueqi Sun [a], Shujing Feng [a], Lei Zhang [a], Jinliang Xu [b], Zheng Miao [b]

[a] Hebei Key Laboratory of Low Carbon and High Efficiency Power Generation Technology, North China Electric Power University, Baoding 071003, Hebei, China
[b] Key Laboratory of Power Station Energy Transfer Conversion and System, North China Electric Power University, Ministry of Education, 102206 Beijing, China

ARTICLE INFO

Keywords:
Organic Rankine cycle
Supercritical pressure extraction
Compression regeneration
Performance analysis
Cycle splitting method

ABSTRACT

The regeneration process is a crucial factor in enhancing the thermal efficiency of an organic Rankine cycle (ORC). This study introduces a novel approach called the supercritical organic Rankine cycle (S-ORC), which utilizes extraction steam compression regeneration in the supercritical state. This breakthrough addresses the existing limitation of subcritical pressure regeneration in ORC research. The study involved the construction of two configurations: the S-ORC and the supercritical regeneration ORC (SR-ORC), which incorporates turbine exhaust regeneration. The working fluid employed for both cycles was R245fa. The thermal efficiency of the S-ORC increased from 17.86 % to 18.85 %, and its exergy efficiency increased from 46.23 % to 48.79 %. Similarly, the thermal efficiency of the SR-ORC increased from 22.66 % to 23.49 %, and its exergy efficiency increased from 58.65 % to 60.8 %. Using the thermal cycle splitting method, we analyzed the S-ORC and found that it can be considered a superposition of an ORC and a single-regeneration Brayton cycle. The equivalent cooling process of the Brayton cycle did not release heat into the environment but rather transferred it to the mainstream of the ORC through regenerative processes. This resulted in an efficiency increase, as the network of the Brayton cycle is equivalent to ± 1. When the network was greater than zero, the S-ORC was superimposed on top of the network of the ORC, thereby increasing overall efficiency. This explains the mechanism behind the enhanced efficiency of the S-ORC. Furthermore, by examining the essential parameters of the cycle and considering various working fluids, we further demonstrated the efficiency advantage of the S-ORC. This study explored the regeneration potential in the supercritical region and proposed an ORC based on compression regeneration in the supercritical state. The proposed approach significantly improves the thermal efficiency of the cycle and achieves structural optimization.

1. Introduction

The organic Rankine cycle (ORC) has gained significant attention in the field of low-grade thermal energy generation due to its simple structure, low cost, high safety, and low maintenance [1–3]. It has found practical applications in various domains, including solar energy [4,5], geothermal energy [6,7], biomass [8,9], and industrial waste heat [10,11]. However, a major drawback of the ORC is its limited operating temperature range, which results in low system efficiency [12]. As a result, enhancing the efficiency of the ORC has emerged as a crucial research objective. Extensive analysis has been conducted to investigate key parameters and optimize the cycle's structure [13,14], aiming to improve its overall efficiency.

According to thermodynamic analysis, the use of supercritical parameters in the ORC offers several advantages, including higher thermal efficiency and increased power output [15–17]. This is primarily due to the improved matching between the working fluids and the low- to medium-temperature heat sources achievable with supercritical parameters. Yu et al. [18] demonstrated that the area enclosed by the heat source temperature change curve and the cycle heat absorption curve are proportional to the heat loss. At the same main vapor temperature, operating at supercritical conditions, which allow for continuous changes in physical properties without passing through the two-phase region, decreases the enclosed area of the heat absorption process of the cycle and the heat release process of the heat source compared to operation at subcritical conditions. Consequently, the efficiency of the

* Corresponding author at: Hebei Key Laboratory of Low Carbon and High Efficiency Power Generation Technology, North China Electric Power University, Baoding 071003, Hebei, China.
E-mail address: ehsun@ncepu.edu.cn (E. Sun).

https://doi.org/10.1016/j.enconman.2023.117546
Received 4 July 2023; Received in revised form 7 August 2023; Accepted 12 August 2023

ORC operating at supercritical parameters is higher.

Numerous studies have been conducted to compare the performance of ORCs under supercritical and subcritical conditions, consistently demonstrating the superiority of supercritical parameter cycles. Li et al. [19] compared the performance of subcritical and supercritical cycles using R1234ze(E) as the working fluid. Although the supercritical parameters were found to be less economically favorable, they resulted in higher cycle thermal efficiency and a maximum net output power increase of 18.2 %. Yağli et al. [20] designed subcritical and supercritical ORCs utilizing engine exhaust flue gas waste heat as the heat source. By varying the turbine inlet temperature and pressure, they analyzed system net power, total pump power consumption, thermal efficiency, and exergy efficiency, concluding that the supercritical ORC outperformed the subcritical ORC with improvements of 2.29 kW in net power and 0.42 % in thermal efficiency. Zabek [21] et al. created a system design for a supercritical cycle with the objective of maximizing net power output. The advantages of the supercritical cycle were particularly prominent for heat sources without outlet temperature limitations or regeneration, with net power output differences of up to 200 kW observed between ambient temperatures of 10 °C and 28 °C under the same design conditions. Maraver [22] investigated the efficiency optimization of subcritical and supercritical cycles with different heat sources and working fluids. The results showed that the supercritical cycle exhibited fewer irreversible losses, and R245fa demonstrated higher exergy efficiencies of 47.6 % and 50.3 % for two outlet temperature-limited heat sources, respectively. In conclusion, the use of supercritical parameters in the ORC offers significant performance advantages compared to subcritical conditions, including higher efficiency and improved power output.

For cycle structure optimization, most existing studies are centered on regeneration methods. Regeneration optimization in the cycle structure can be categorized into two methods: turbine exhaust regeneration, which utilizes the high-temperature working fluid from the turbine exhaust to heat the mainstream working fluid, and extraction steam regeneration, which achieves regeneration by extracting steam from the turbine intermediate stage [23–25]. In their study, Imran et al. [26] utilized geothermal energy as a low-temperature heat source to construct a basic, a turbine exhaust regenerative, and an extractive regenerative ORC. The results indicated that turbine exhaust regeneration significantly improved the ORC's exergy efficiency by 4.03 % compared to the basic ORC. Additionally, the use of an extractive regenerative structure reduced the heat load on the condenser. Several studies have compared turbine exhaust regeneration with basic supercritical ORCs. Feng et al. [27] conducted a comparative study based on a 10 kW ORC experimental prototype using R245fa working fluid, examining both basic (BORC) and turbine exhaust regenerative (RORC) cycles. The results demonstrated a 1.7 % improvement in the thermal efficiency of RORC over BORC. Yağlı et al. [28] designed basic and turbine exhaust regeneration ORCs that utilized biogas as the driving heat source. They optimized and compared the performance of the turbine exhaust regeneration ORC, which exhibited superior results, achieving a maximum net power of 45.3 kW, thermal efficiency of 12.34 %, and exergy efficiency of 68.02 %. Le et al. [29] employed a genetic algorithm to maximize the efficiency of various working fluid systems at a turbine inlet temperature of 139 °C. The study aimed to optimize cycle thermal and exergy efficiencies, which were found to be 16 % and 59 %, respectively. The results indicated that the regenerative structure significantly improved the system efficiency when combined with the supercritical ORC. Braimakis et al. [30] designed and compared the performance of three dual-pressure regenerative ORCs based on turbine exhaust regeneration. They analyzed the effect of high-pressure turbine outlet pressure on cycle performance and found that the dual-pressure and dual-turbine exhaust regenerative ORCs exhibited the best performance. Without turbine exhaust regeneration, the maximum efficiency reached 20.9 %, while with turbine exhaust regeneration, the maximum efficiency increased to 24.5 %.

From the perspective of both key cycle parameters and structural optimization, supercritical ORC coupling regeneration represents a direction for enhancing ORC efficiency. However, current studies on the regeneration of ORCs mainly focus on regenerating superheated steam at subcritical pressure. This raises the question: Is there potential for further improvement in cycle regeneration optimization? To address this question, this study proposes an innovative approach by introducing compression regeneration in the supercritical state within an ORC (S-ORC), which offers a promising avenue for improving efficiency. The study analyzes the system's performance using thermodynamic principles and explores the impact of key cycle parameters and various working fluids, providing further evidence for the efficiency advantages of the proposed approach.

2. System construction and calculation methods

2.1. Basic ORC thermodynamic model

Fig. 1 shows a schematic and *T-s* diagram of a supercritical basic ORC system and a supercritical basic ORC coupled with turbine exhaust regeneration (Fig. 1(a)). The cycle consisted of a turbine, condenser, work mass pump, and evaporator. For a non-regenerative supercritical ORC cycle, 1–2 is the working expansion of organic working fluid in the turbine; 2–3 is the cooling process after the fluid enters the condenser; 3–4 is the compression process of the fluid by the pump; and 4–1 is the heat absorption process of the fluid finally entering the evaporator after pressurization, which completes a thermal cycle. Fig. 1(b) shows a supercritical basic ORC coupled with turbine exhaust regeneration (R-ORC). This cycle adds a recuperator at the turbine outlet to preheat the fluid at the pump outlet section by using the residual heat of the spent steam, thus raising the temperature of the fluid when it enters the evaporator, reducing the heat absorption of the fluid in the evaporator and improving cycle efficiency.

The thermodynamic calculations were conducted using a custom program developed in Fortran. The circulating working fluid chosen for the analysis was R245fa, and the corresponding physical parameters were obtained from REFPROP 9.1 [31]. To simplify the thermodynamic calculations, the system was assumed to operate stably, and the heat loss to the environment except for that of the cooler and the pressure loss in the piping of each component were ignored. The relevant calculation parameters of the circulation system are listed in Table 1, and the specific calculation model can be expressed as follows.

According to the conservation of energy, the total heat input into the cycle evaporator is:

$$Q_{\mathrm{ORC}} = m_{\mathrm{wf}}(h_1 - h_4) = m_{\mathrm{hs}}\left(h_{\mathrm{hs,in}} - h_{\mathrm{hs,out}}\right) \tag{1}$$

where Q_{ORC} is the system heat absorption; h_1 and h_4 are the inlet enthalpy of the turbine and evaporator, respectively; m_{wf} is the mass flow rate of the working fluid; m_{hs} is the mass flow rate of the heat source; and the subscript in/out indicate the inlet and outlet.

The isentropic efficiency ($\eta_{\mathrm{T,s}}$) and output power of the turbine (W_{T}) are:

$$\eta_{\mathrm{T,s}} = \frac{h_1 - h_2}{h_1 - h_{2,\mathrm{s}}},\ W_{\mathrm{T}} = m_{\mathrm{T}}(h_1 - h_2) \tag{2}$$

where h_1, $h_{2,\mathrm{s}}$, and h_2 are the inlet enthalpy, isentropic outlet enthalpy, and actual outlet enthalpy of the turbine, respectively; and m_{T} is the mass flow rate of the working mass in the turbine.

The isentropic efficiency of the pump ($\eta_{\mathrm{P,s}}$) and its power consumption (W_{P}) are:

$$\eta_{\mathrm{P,s}} = \frac{h_{4,\mathrm{s}} - h_3}{h_4 - h_3},\ W_{\mathrm{P}} = m_{\mathrm{P}}(h_4 - h_3) \tag{3}$$

where h_3, $h_{4,\mathrm{s}}$, and h_4 are the inlet enthalpy, isentropic outlet enthalpy,

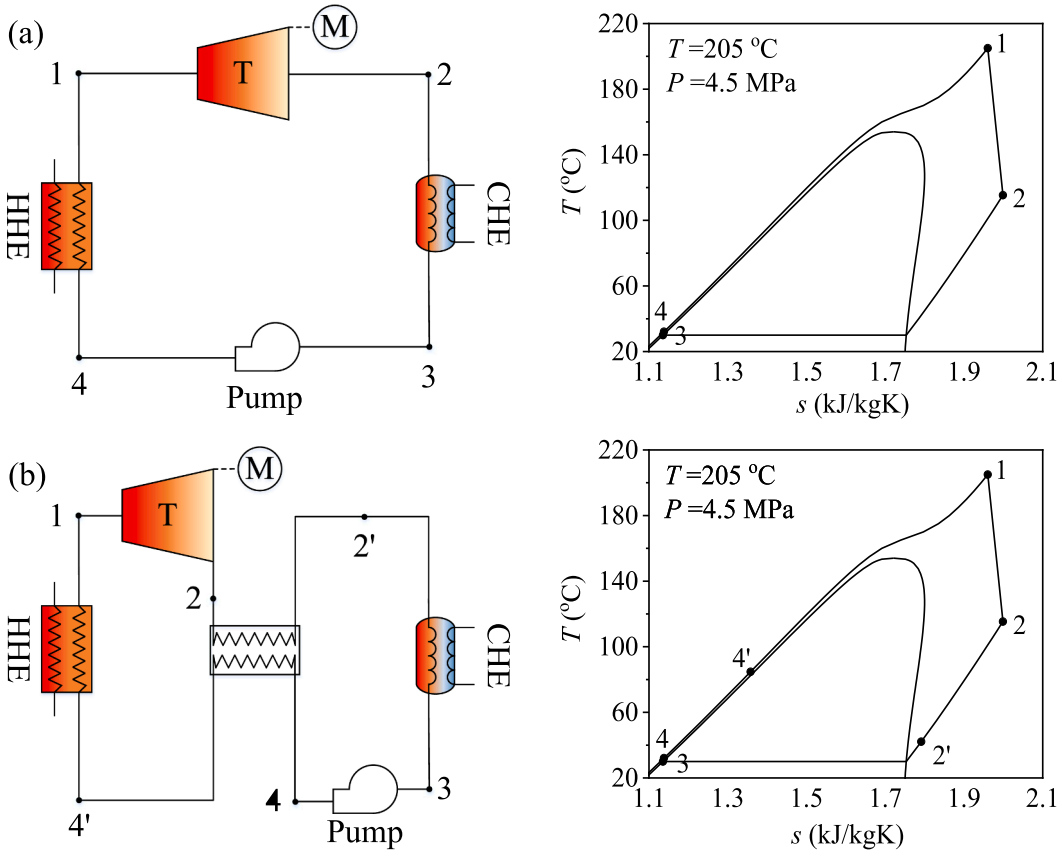

Fig. 1. ORC(a)/R-ORC(b) process flow diagram and *T-s* diagram.

Table 1
Cycle calculation assumptions.

Parameter	Value
Environmental temperature, T_0 (°C)	20
Environmental pressure, p_0 (kPa)	101.325
Heat source temperature, $T_{hs,in}$ (°C)	230
Type of the working fluid	R245fa
Turbine isentropic efficiency, η_T (%)	85[35,36]
Pump isentropic efficiency, η_P (%)	8[37,38]
Compressor isentropic efficiency, η_C (%)	83
Pinch point in evaporator ΔT_e (°C)	10[35,36]
Pinch point in condenser ΔT_c (°C)	5[35,36]
Pinch point in regenerator ΔT_{reg} (°C)	10[39,40]
Condensing temperature, T_{cd} (°C)	30[41,42]

and actual outlet enthalpy of the work mass pump, respectively; and m_P is the mass flow rate of the work mass in the pump.

The cycle thermal efficiency is:

$$\eta_{th} = \frac{W_T - W_P}{Q_{ORC}} \tag{4}$$

For the evaporator, the state point-specific exergy at the inlet and outlet of the heat source is:

$$e_{hs,in} = \left(h_{hs,in} - h_0\right) - T_0\left(s_{hs,in} - s_0\right) \tag{5}$$

$$e_{hs,out} = \left(h_{hs,out} - h_0\right) - T_0\left(s_{hs,out} - s_0\right) \tag{6}$$

Then the total input exergy value of the system is:

$$E_{hs} = m_{hs}\left(e_{hs,in} - e_{hs,out}\right) \tag{7}$$

The second law efficiency of the cycle can be defined by the ratio of the network output to the total (exergy) input through the evaporator, expressed as:

$$\eta_{II} = \frac{W_T - W_P}{E_{hs}} \tag{8}$$

2.2. ORC with extraction steam compression regeneration in the supercritical state

To further enhance the average heat absorption temperature and improve the thermal efficiency of the cycle, this study introduced the concept of the S-ORC. The S-ORC capitalizes on the regeneration potential within the supercritical cycle. Fig. 2 illustrates the flow diagram and corresponding *T-s* diagram of the S-ORC. Fig. 2(a) presents the S-ORC derived from the basic ORC depicted in Fig. 1(a). The supercritical state extraction steam compression regeneration process consisted of two recuperators and a compressor. Initially, extraction is performed from the intermediate stage of the turbine, where the fluid is extracted at supercritical pressure. It then enters the compressor after preheating the main fluid through two recuperators, followed by compression and mixing with the main fluid at 7-point. Subsequently, the mixture enters the first recuperator H1 and proceeds to the evaporator to continue the cycle. Fig. 2(b) displays the flow and *T-s* diagrams (referred to as SR-ORC) of the supercritical state extraction steam compression regeneration process applied based on the turbine exhaust regeneration ORC.

In the thermodynamic model of the ORC coupled with compression regeneration in the supercritical state, the calculation process is similar to that of the basic cycle described in Section 3.1, with the addition of the compressor power consumption equation. All other equations remain the same.

The isentropic efficiency of the compressor ($\eta_{C,s}$) and its power consumption (W_C) are:

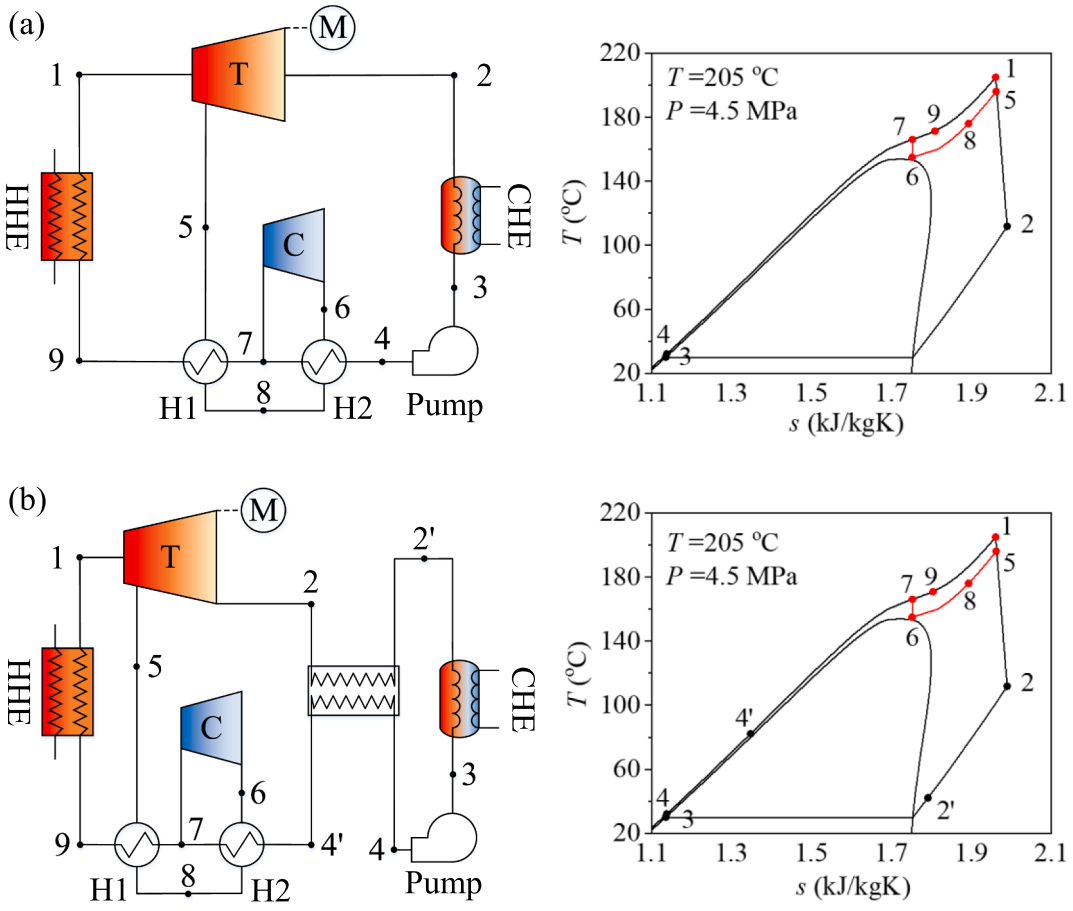

Fig. 2. S-ORC(a)/SR-ORC(b) process flow diagram and *T-s* diagram.

$$\eta_{C,s}=\frac{h_{7,s}-h_6}{h_7-h_6},\ W_C=m_C(h_7-h_6) \tag{9}$$

where h_6, $h_{7,s}$, and h_7 are the inlet enthalpy, isentropic outlet enthalpy, and actual outlet enthalpy of the compressor, respectively; and m_C is the mass flow rate of the working mass in the compressor.

Due to the significant changes in physical properties of the organic working fluid near the critical region, it is important to consider the specific heat transfer process inside the recuperator to address the potential issue of pinch point temperature differences in the H2 section of both the S-ORC and SR-ORC. The temperature on the low-pressure side of the H2 gradually converges to the critical temperature, leading to a non-linear trend in fluid temperature variation on both the high- and low-pressure sides of the recuperator. To mitigate this, the heat transfer process inside the recuperator is calculated to ensure that the temperature difference between the pinch point of the H2 remains at a constant 10 °C in all operating conditions, thus avoiding any temperature-related issues [32]. Fig. 3 illustrates the *T-Q* diagram within the H2 recuperator of the S-ORC and SR-ORC, clearly demonstrating the non-linear behavior of the fluid temperature on both sides of the recuperator.

Using the calculation method described in this study, the thermodynamic first and second law efficiencies were derived for each of the

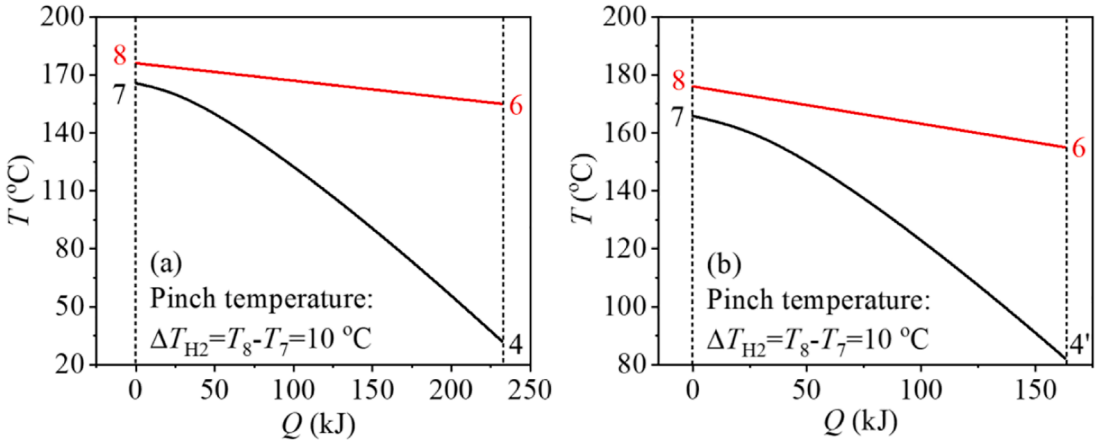

Fig. 3. *T-Q* plot of H2 in S-ORC(a) and SR-ORC(b).

four cycles, considering the main temperature and pressure parameters of 205 °C and 4.5 MPa (R245fa: T_{cp} = 154.01 °C, P_{cp} = 3.651 MPa), as shown in Fig. 4. It was evident that the cycle efficiency experienced a significant increase when coupled with the supercritical state compression regeneration compared to the reference cycles. Specifically, the S-ORC exhibited a thermal efficiency improvement of 1.29 % and an exergy efficiency increase of 3.3 % over the ORC, while the SR-ORC demonstrated a thermal efficiency improvement of 1.0 % and an exergy efficiency increase of 2.8 % over the R-ORC. These results highlight the substantial cycle efficiency enhancement achieved through the supercritical state extraction steam compression regeneration process.

As depicted in Fig. 5(a) and (c), the introduction of coupled turbine exhaust regeneration (R-ORC) into the basic ORC led to a significant 10.25 % and 7.3 % reduction in exergy loss in the evaporator and condenser, respectively. This improvement is attributed to the utilization of waste heat from the spent steam, which raises the average heat absorption temperature and lowers the average heat release temperature, resulting in enhanced exergy efficiency of the system.

Fig. 5(b) and (d) demonstrate that the system's exergy efficiency was further enhanced by introducing the supercritical state extraction steam compression regeneration process on top of the ORC and R-ORC. This improvement was primarily observed in two aspects. Firstly, the exergy loss in the evaporator of each component was significantly reduced, accounting for only 1.77 % (S-ORC) and 2.2 % (SR-ORC) of the total input exergy. This reduction is attributed to the supercritical state extraction steam compression regeneration process, which raises the average heat absorption temperature closer to the heat source's set temperature, resulting in better matching between the main evaporation section and the heat source. Secondly, the introduction of steam extraction reduced the flow rate of the turbine, condenser, and pump, leading to a significant decrease in the corresponding exergy losses of these components. However, the increase in power consumption of the compressor and the heat regeneration from the recuperator offset this reduction. As a result, the maximum exergy loss in the two new cycles was transferred from the evaporator and condenser in the ORC/R-ORC to the high-temperature recuperator H2 and the compressor.

Based on the above analysis, after coupling the supercritical state extraction steam compression regeneration process (S-ORC/SR-ORC), the cycle structure was further optimized. This begs the question: what then is the mechanism by which the supercritical state extraction steam compression regeneration process enhances cycle efficiency? We examine this question in Section 2.3.

2.3. Cycle feasibility analysis

The cycle thermal efficiency relationship between the S-ORC and basic ORC can be derived by applying the first law of thermodynamics. This reveals the mechanism by which the supercritical state extraction steam compression regeneration process enhances cycle thermal efficiency. The total flow rate was set as $(1+\alpha)$ kg/s, and α is the extraction flow rate of the supercritical state extraction steam compression regeneration process.

Neglecting the heat loss of the recuperator, the heat balance equation for recuperators H1 and H2 in the S-ORC are:

$$h_7 - h_4 = \alpha(h_8 - h_6) \tag{10}$$

$$(1+\alpha)(h_9 - h_7) = \alpha(h_5 - h_8) \tag{11}$$

Furthermore:

$$h_9 = \frac{\alpha}{1+\alpha}(h_5 - h_6) - \frac{(h_7 - h_4)}{1+\alpha} + h_7 \tag{12}$$

The work done by the organic working fluid in the turbine can be divided into two parts: (1) the work done by the flow rate of 1 kg/s fluid expanding from 1-point to 2-point, and (2) the work done by the remaining flow rate α kg/s fluid expanding from 1-point to 5-point, see Fig. 2. Therefore, the net cycle power can be expressed as:

$$w = (h_1 - h_2) - (h_4 - h_3) + \alpha(h_1 - h_5) - \alpha(h_7 - h_6) \tag{13}$$

The heat absorbed by the fluid in the evaporator is:

$$q = (1+\alpha)(h_1 - h_9) \tag{14}$$

Together with equation (12) this gives:

$$q = (h_1 - h_4) + \alpha(h_1 - h_5) - \alpha(h_7 - h_6) \tag{15}$$

The thermal efficiency of the cycle can be calculated from the network and heat absorption, giving:

$$\eta_{th}^{'} = \frac{w}{q} = \frac{(h_1 - h_2) - (h_4 - h_3) + \alpha(h_1 - h_5) - \alpha(h_7 - h_6)}{(h_1 - h_4) + \alpha(h_1 - h_5) - \alpha(h_7 - h_6)} \tag{16}$$

For an ORC without regeneration, the cycle thermal efficiency is:

$$\eta_{th} = \frac{(h_1 - h_2) - (h_4 - h_3)}{(h_1 - h_4)} \tag{17}$$

Comparing equations (16) and (17), we can see that the cycle thermal efficiency increases $\eta_{th}^{'} > \eta_{th}$ when $\alpha(h_1 - h_5) - \alpha(h_7 - h_6) \rangle 0$. Where $\alpha(h_1 - h_5) - \alpha(h_7 - h_6)$ represents the difference between the work done by the turbine and the work consumed by the compressor of the supercritical state compression regeneration part, i.e., the network of the supercritical state extraction steam compression regeneration process. Thus, the gain effect of this process on the cycle thermal efficiency is reflected in the basic ORC superimposed on part of the network, that is, by superimposing the network on the basic organic Rankine cycle, the thermal efficiency of the S-ORC must be higher than the thermal efficiency of the ORC. According to the network expression, the network is

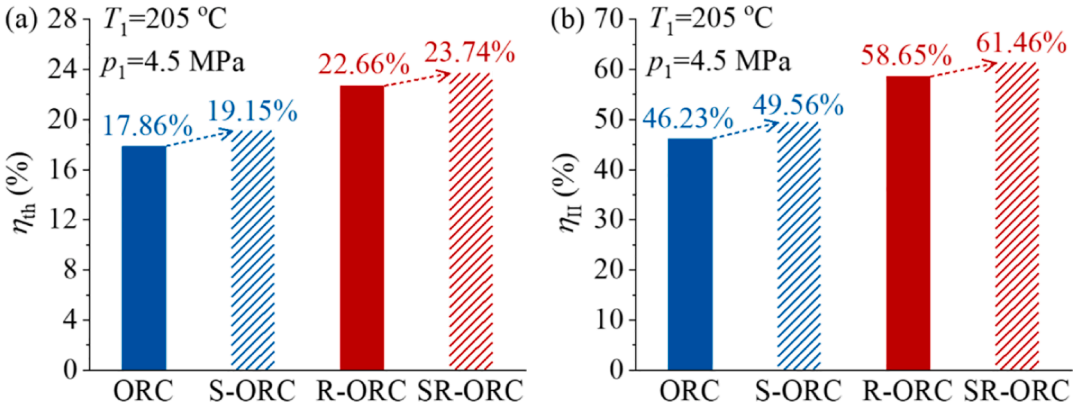

Fig. 4. Comparison of cyclic thermal efficiency (a) and second law efficiency (b) of four cycles.

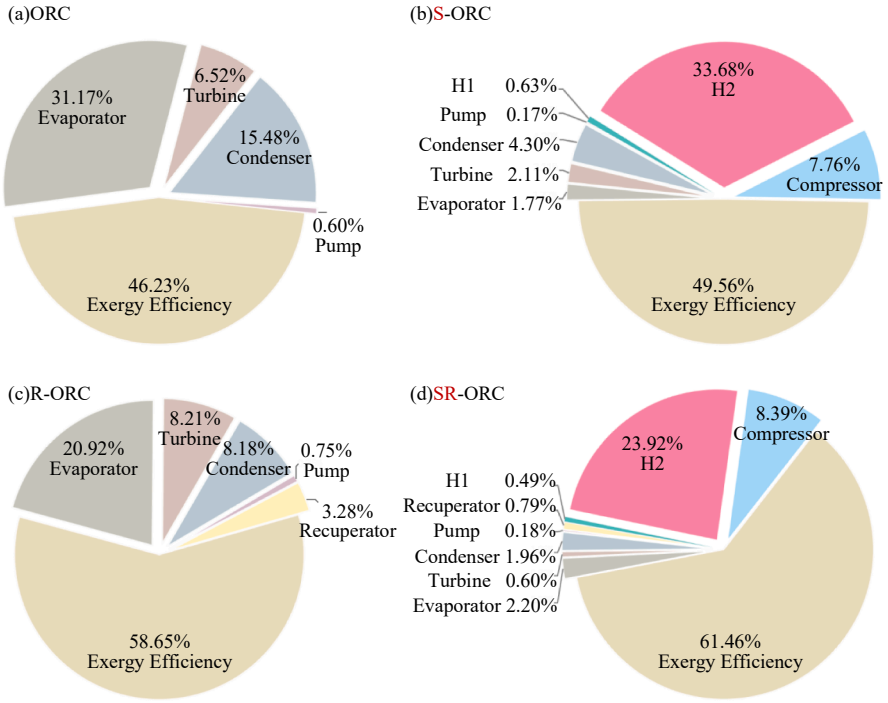

Fig. 5. Graph of the proportion of exergy loss by each component in the four cycles.

mainly affected by the extraction flow rate α, the extraction enthalpy h_5, the compressor inlet enthalpy h_6, and the compressor outlet enthalpy h_7. Additionally, $\alpha = \frac{h_7 - h_4}{h_8 - h_6}$, h_7 can be obtained based on the compressor isentropic efficiency. Therefore, the effect of the supercritical state extraction steam compression regeneration process on cycle thermal efficiency is mainly influenced by the following parameters:

$$\eta_{th}^{'} = f(P_5, T_6, \Delta T_{H2}, \eta_C) \tag{18}$$

where P_5 is the extraction pressure, T_6 is the compressor inlet temperature, ΔT_{H2} is the pinch temperature of recuperator H2, and η_C is the compressor isentropic efficiency. That is, the closer the compressor inlet is to the critical point, the smaller the recuperator pinch point temperature difference. Similarly, the higher the compressor isentropic efficiency, the more significant the effect of the supercritical state extraction steam compression regeneration process on efficiency improvement.

However, some potential uncertainties, experimental biases, and practical challenges may exist in implementation. First, in practice, the inlet parameter of the compressor is set as close as possible to the critical point of the working fluid to maximize the network of the equivalent Brayton cycle. However, at this time, it is prone to condensation phenomenon at the leading edge of the impeller, which brings potential uncertainty to the safe operation of the compressor.

Second, in the experimental operation, ensuring that the ratio of extraction diversion in the supercritical state extraction steam compression regeneration process agrees with the theoretical calculations is necessary. The temperature and pressure should be the same at the convergence point of different flow rates, which is more difficult to realize and may cause a deviation between the experimental results and the theoretical calculations.

Finally, in practice, the constraints between cycle efficiency and increased cost should be considered owing to the increase in the corresponding mass flow rate of the supercritical state extraction steam compression regeneration process and the addition of compressor and recuperator components.

In addition to the quantitative derivation of the first law of thermodynamics, the effectiveness of the supercritical state extraction steam compression regeneration process can also be demonstrated through the cycle splitting method [33,34]. The assumptions before the analysis are as follows: first, in the splitting process, we assume S-ORC to be the base cycle and an equivalent cycle. Second, we set the temperature and pressure parameters at the point of convergence of different flow phases in the cycle to be similar, i.e., there is no loss of energy and exergy in the convergence process. Finally, the assumed compressor inlet parameter in this study tends to be close to the critical point of the work fluids to reduce the compressor dissipation and improve the cycle efficiency.

Fig. 6 illustrates the S-ORC construction process based on the splitting method. The analysis begins by decoupling the S-ORC into two independent cycles: the basic ORC (6b) and the organic working fluid Brayton cycle (6c). In this configuration, the heat released from process 8–6, prior to entering the compressor in the Brayton cycle, is exchanged with the pump outlet section 4–7 in the ORC through the recuperator H2 to achieve regeneration, rather than released into the environment. This process is equivalent to overlaying a cycle with an efficiency equivalent to 1 on top of the basic cycle. The *T-s* diagram of the cycle analyzed using the cycle splitting method is presented in Fig. 7. It demonstrates that the S-ORC can be considered a superposition of the basic ORC and the supercritical compression regeneration cycle, and that the equivalent efficiency of this cycle is 1. After the supercritical state extraction and compression regeneration process is superimposed, the cycle exhibits significantly higher average heat absorption temperatures and thermal efficiency compared to the basic cycle. The mechanism of action of the supercritical state extraction steam compression regeneration process is visually better represented from the perspective of the cycle splitting method, which aligns with the results derived from the first law of thermodynamics, indicating that the process achieves efficiency improvement by adding a network on top of the basic cycle.

However, the splitting method still has some limitations: First, whether the splitting method is suitable for subcritical cycles needs further study. Second, the application of the splitting method in this paper analyzes pure fluid cycles. For other systems, such as flash-based

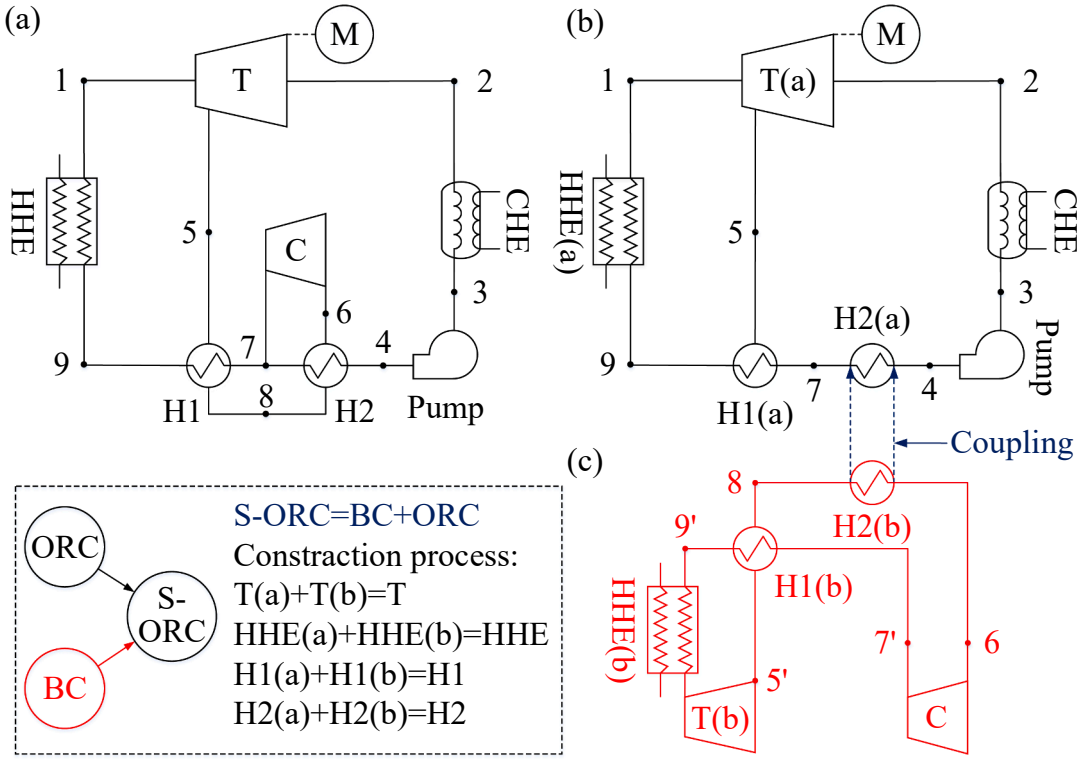

Fig. 6. Construction of the S-ORC based on the thermal cycle splitting method.

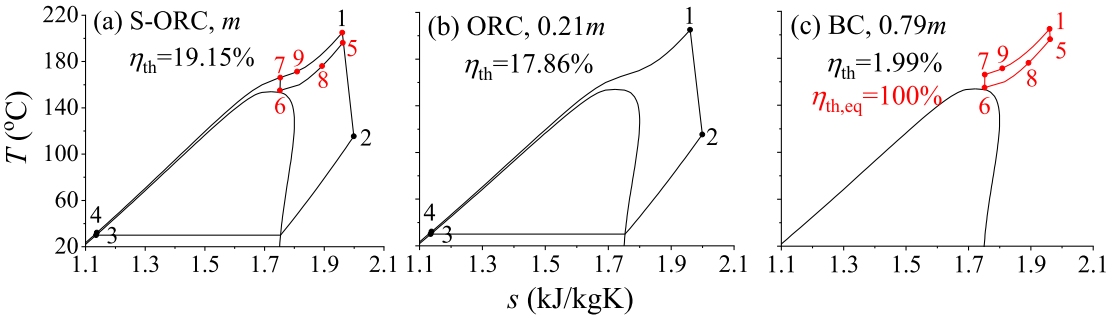

Fig. 7. Schematic of the S-ORC splitting.

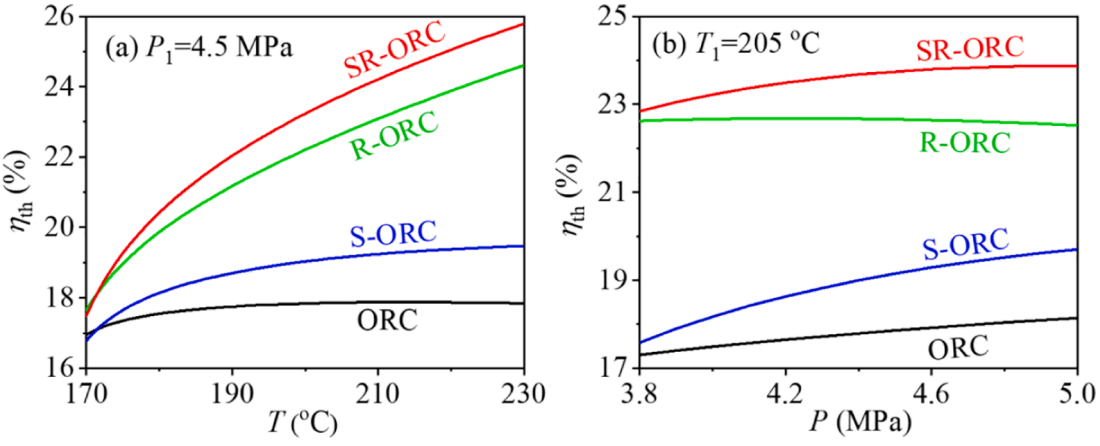

Fig. 8. Effect of main vapor parameters on cycle thermal efficiency.

systems or ORCs with mixed fluids, whether the splitting method is applicable needs to be further explored owing to phenomena such as phase separation. Finally, the applicability of the splitting method to some systems that include chemical reactions or phase changes, such as chemical chain cycles and lithium bromide refrigeration, also needs to be investigated.

3. Results and discussions

3.1. Influence of main vapor parameters on S-ORC/SR-ORC system performance

Fig. 8(a) and (b) illustrate the relationship between the turbine inlet main temperature pressure parameter and the thermal efficiency of each of the four ORCs. The S-ORC/SR-ORC exhibited a more significant improvement in thermal efficiency compared to its corresponding basic cycle. However, it is evident that the presence or absence of turbine exhaust regeneration had a notable effect on the trend of thermal efficiency change, as shown in Fig. 8(a). The thermal efficiency of the R-ORC and SR-ORC was more sensitive to temperature changes compared to the cycle without turbine exhaust regeneration.

As shown in Fig. 8(a), the sensitivity of thermal efficiency to temperature change varies among the four cycles, mainly in ORC and S-ORC without turbine exhaust regeneration, where the curves of efficiency versus main vapor temperature are flatter, while the curves of R-ORC and SR-ORC are steeper, a phenomenon that can be analyzed in terms of the average temperature. As shown in Fig. 9, the red line indicates the average temperature at which heat is added ($T_{ave,h}$), and the black line indicates the average temperature at which heat is rejected ($T_{ave,c}$). In the ORC/S-ORC, as the main vapor temperature increases, the $T_{ave,h}$ of the cycle increases, the turbine exhaust temperature increases, and the $T_{ave,c}$ of the cycle increase; owing to the mutual constraints of the two, the thermal efficiency curves of the ORC/S-ORC tends to be flat (Fig. 9a, b). During the coupled turbine exhaust regeneration (Fig. 9c, d), the average temperature at which heat is rejected remains constant, so the thermal efficiency of R-ORC/SR-ORC is more sensitive to the change of the main steam temperature, and its curve is steeper.

Moreover, as shown in Fig. 8(a), the thermal efficiency curves crossed when the main vapor temperature was near 170 °C, and the thermal efficiency of the two new cycles coupled with the supercritical state extraction steam compression regeneration process (S-ORC/SR-ORC) was lower than that of the basic cycle (ORC/R-ORC), with the thermal efficiencies of the ORC and S-ORC at a main vapor temperature of 170 °C being 16.95 % and 16.78 %, and those of the R-ORC and SR-ORC being 17.65 % and 17.49 %, respectively. Notably, this does not contradict the results described in Section 2.3. This phenomenon occurs because the network of the supercritical state extraction steam compression regeneration process, when added to the basic cycle, is negative, thereby reducing the efficiency of the coupled cycle. A comparison of equations (16) and (17) showed that cycle thermal efficiency is higher than the basic cycle only when the work done by the fluid in the turbine is greater than the work consumption in the compressor under the supercritical state extraction steam compression regeneration process. This indicates that the efficiency-enhancing effect of the supercritical extraction and compression regeneration process is dependent on the network of the superposition cycle being greater than zero, which supports the results in Section 2.3. Equations (16) and (17) show that the thermal efficiency of the novel cycle is only affected by $\alpha(h_1 - h_5) - \alpha(h_7 - h_6)$, which is the difference between the equivalent turbine work and the compressor dissipation in the supercritical state extraction steam compression regeneration process, i.e., the network of the coupled equivalent Brayton cycle. When the main vapor parameter is less than a certain threshold, the network of the coupled novel cycle is less than zero, meaning that the network of the coupled novel cycle is lower than that of the original base cycle, which in turn leads to a reduction in the thermal efficiency of the cycle. The intersection point in Fig. 8(a) is where the work done by the turbine is equal to the work dissipated by the compressor at the corresponding flow rate.

It can be observed in Fig. 8(b) that the cycle's thermal efficiency increased as the main vapor pressure rose. For the cycle coupled with the

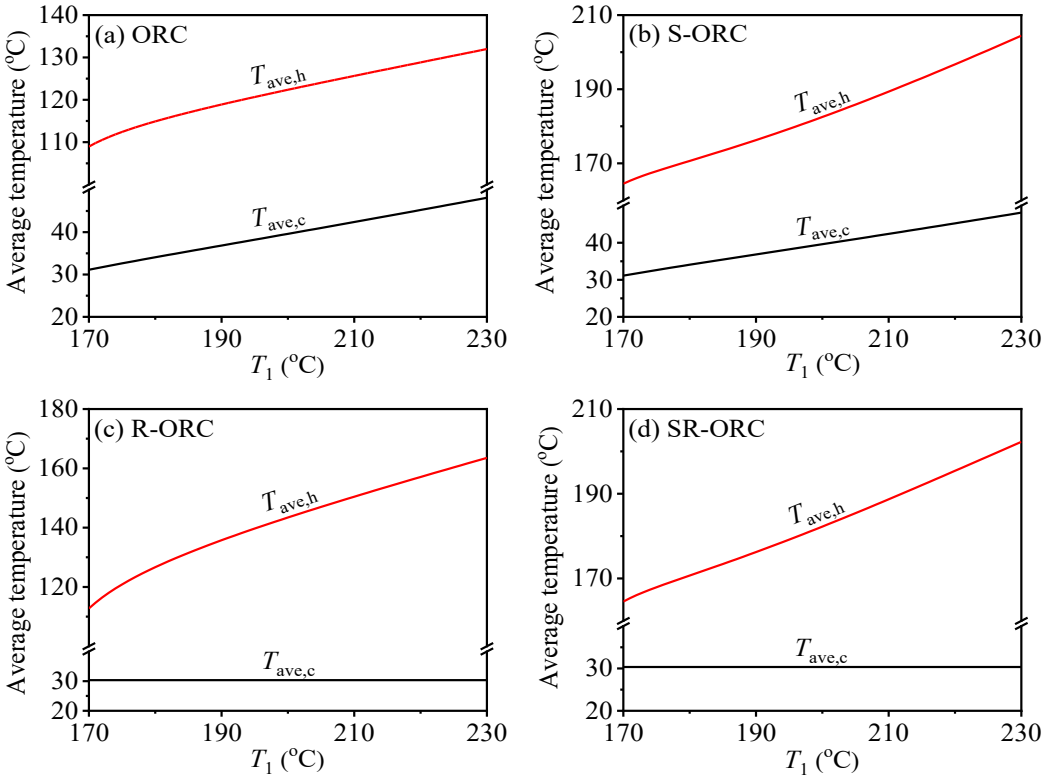

Fig. 9. Average temperature plot for four cycles.

supercritical extraction and compression regeneration process, an appropriate increase in the main vapor pressure benefitted the improvement of cycle efficiency. Furthermore, it is apparent in the figure that as the main vapor pressure approached the critical pressure, the thermal efficiency of the new cycle (S-ORC/SR-ORC) tended to approach that of the corresponding basic cycle (ORC/R-ORC). This is attributed to the selected working fluid, R245fa, having a critical pressure of 3.65 MPa. As the main vapor pressure approaches the critical pressure of the fluid, the network of the cycle coupled with the supercritical state extraction steam compression regeneration process approached zero, resulting in the thermal efficiency of the S-ORC/SR-ORC approaching that of the ORC/R-ORC.

3.2. Influence of the parameters of the extracted vapor on S-ORC/SR-ORC system performance

Fig. 10 illustrates the variation in cycle thermal efficiency for the S-ORC and SR-ORC with different compressor inlet (6-point) parameters in the supercritical state extraction steam compression regeneration process. The figure indicates that the cycle's thermal efficiency for the S-ORC and SR-ORC was higher when the compressor inlet parameter, represented by the 6-point in the *T-s* diagram, see Figs. 6 and 7, was closer to the critical point of the circulating working fluid. For instance, at a compressor inlet parameter of 155 °C/3.7 MPa, the thermal efficiencies were 19.15 % for the S-ORC and 23.74 % for the SR-ORC. However, at a compressor inlet parameter of 165 °C/4 MPa, the thermal efficiencies were 18.38 % and 23.11 %, respectively.

Based on the analyses in Sections 2.3 and 3.1, when the network of the superimposed cycle was greater than zero, the overall cycle's thermal efficiency was improved. Additionally, when the compressor inlet was closer to the critical point of the working fluid, the compressor power consumption decreased, leading to a larger network for the superimposed cycle. Consequently, the cycle's thermal efficiency for the S-ORC and SR-ORC was higher. This explains the trend observed in Fig. 10.

Fig. 11 illustrates the trend of the extraction flow rate for the S-ORC and SR-ORC as a function of the parameters of the compressor inlet (6-point) in the supercritical state extraction steam compression regeneration process. In the calculation, the total cycle flow rate is assumed to be a unit mass flow rate, and the graph presents the proportion of the extraction flow rate to the overall total cycle flow rate. The trend indicates that when the parameter T_6 was determined and the compressor inlet pressure P_6 was changed, there was no significant change in the extraction flow rate. Conversely, when the parameter P_6 was determined and the compressor inlet temperature T_6 was changed, the extraction flow gradually increased with the increase in T_6.

Based on the analysis in Section 2.3, illustrated in Figs. 10 and 11, we believe that, when superimposing the supercritical state extraction steam compression regeneration process, the closer the 6-point parameter, i.e., the compressor inlet point, is to the critical point of the circulating working fluid, the better the superimposition effect, the higher the overall cycle thermal efficiency, and the more optimal the overall system performance.

3.3. System thermal efficiency of the S-ORC/SR-ORC under different cycle working fluids

To further verify the advantages of the proposed supercritical state extraction steam compression regeneration process, nine different organic fluids, including R245fa, were selected for analysis. The characteristic parameters of each type of organic fluid are listed in Table 2. Furthermore, Fig. 12 shows the efficiency curves of these fluids at different temperature conditions. The four cycles were divided into two groups: with or without turbine exhaust regeneration. The efficiency curves of the ORC/S-ORC and R-ORC/SR-ORC at different circulating fluid conditions with main vapor temperatures are shown in Fig. 12(a) and (b), respectively. To ensure that the network of the novel cycle, as shown in Fig. 8, remained greater than zero, the cycle was divided into different temperature intervals based on the characteristics of the different fluids and the temperature threshold conditions. The results indicated that for design temperatures below 160 °C, fluids such as R227ea and R1234ze can be utilized. In this case, the thermal efficiency of the S-ORC could achieve values of 14.5 % and 15.22 %, while that of the SR-ORC could reach efficiencies of 17.58 % and 17.15 % at a main vapor parameter of 150 °C/4.5 MPa. However, R227ea was selected as preferable owing to the highly flammable nature of R1234ze. Conversely, for design temperatures above 160 °C, fluids like R245fa and R123 can be employed. At a main vapor parameter of 220 °C/4.5 MPa, the S-ORC achieved thermal efficiencies of 19.38 % and 21.74 %, whereas the SR-ORC could attain efficiencies of 25.05 % and 24.79 %. Based on the higher toxicity of R123, R245fa was a better choice in comparison. However, the following factors should also be considered in practical applications. In the practical application of ORC power generation, the heat source characteristics are crucial for cycle screening, e.g., for geothermal energy, the applicable ORC fluids will be different for different temperature zones. In addition, the stability, safety, and environmental friendliness of the working fluid are basic and important issues, such as the toxicity, flammability, and ozone depletion of different working fluids.

The calculation based on the first law of thermodynamic demonstrated that the supercritical extraction compression regenerative ORC is equally effective in enhancing the cycle thermal efficiency when driven by different organic working fluids. This indicates the universality of the supercritical state extraction steam compression regeneration process in the field of ORC applications.

We believe that the main challenges and limitations in the

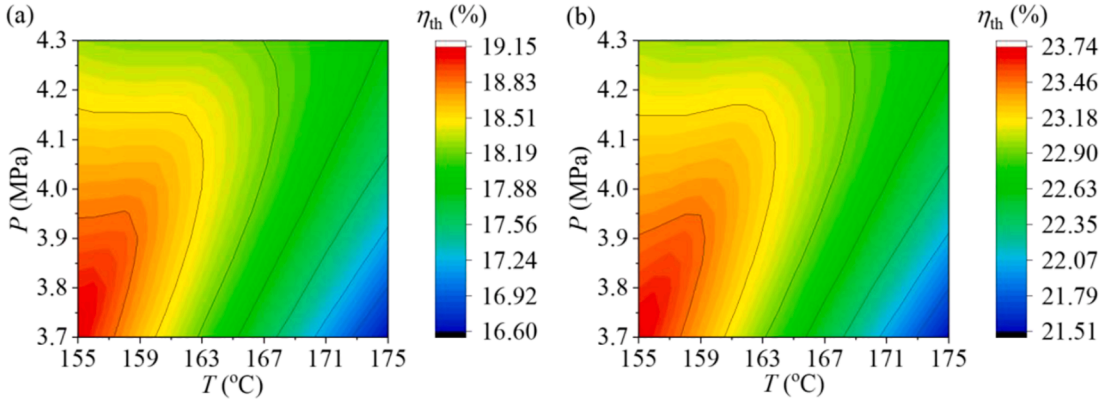

Fig. 10. Effect of vapor extraction parameters on the thermal efficiency of the S-ORC(a)/SR-ORC(b) cycle.

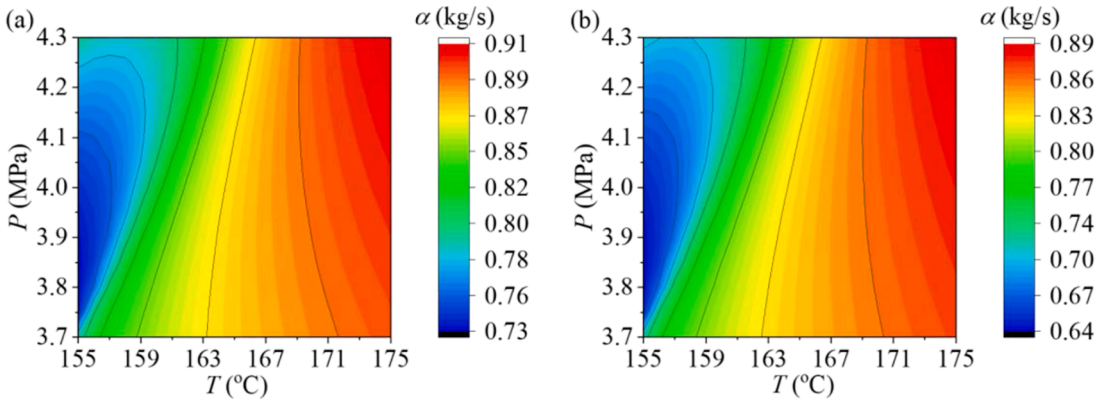

Fig. 11. Effect of vapor extraction parameters on the extraction flow rate.

Table 2
The working fluid properties [43,44].

Working Fluid	Formula	T_c (°C)	P_c (MPa)	GWP	Toxicity	Flammability
R125	C2HF5	66.02	3.618	3170	/	none
R143a	C2H3F3	72.71	3.762	4800	low	highly
R1234yf	C3F4H2	94.70	3.382	< 1	none	highly
R134a	C2H2F4	101.06	4.059	1300	low	none
R227ea	C3HF7	101.75	2.925	3500	low	none
R1234ze	C3F4H2	109.36	3.635	< 1	none	highly
Isobutane	C4H10	134.66	3.629	20	low	extremely
R245fa	C3H3F5	154.01	3.651	858	none	extremely
R123	C2HCl2F3	183.68	3.66	79	high	none

application of this technology are as follows:

To improve the cycle efficiency, the cycle makes the inlet parameter of the compressor as close as possible to the critical point of the working fluid to reduce the compressor power dissipation; however, at this time, it is prone to condensation at the leading edge of the impeller, which poses a challenge to the safe operation of the compressor [45,46]. This point needs to be further considered in practical applications. In addition, the supercritical state extraction steam compression regeneration process requires additional recuperators and compressors, so the cycle may face constraints between cost and efficiency.

Furthermore, when coupled with the supercritical state extraction steam compression regeneration, the degree of regeneration of the cycle increases, and the heat absorption temperature zone in the heat source becomes narrower. Therefore, the cycle is more suitable for combining with heat sources such as solar, geothermal, and nuclear energy but not for combining with flue gas waste heat; therefore, there are some limitations on the selection of heat sources for this cycle.

4. Conclusions

This study introduced the application of the supercritical state extraction steam compression regeneration process to ORCs. The analysis employed the first and second laws of thermodynamics and the cycle splitting method to examine the cycle's structural characteristics and the influence of key factors on its performance. The following conclusions were drawn:

(1) S-ORC and SR-ORCs were developed based on the supercritical state extraction steam compression regeneration process. When R245fa was utilized as the working fluid, the S-ORC demonstrated an increase in cycle thermal efficiency from 17.86 % to 19.15 % and exergy efficiency from 46.23 % to 49.56 % compared to the ORC. Similarly, the SR-ORC exhibited an improvement in cycle thermal efficiency from 22.66 % to 23.74 % compared to R-ORC, along with an increase in exergy efficiency from 58.65 % to 61.46 %, reflecting the efficiency advantages of the new cycle.

(2) The higher thermal efficiency of the new cycle compared to the basic ORC were explained theoretically through thermodynamic derivation. The supercritical state extraction steam compression regeneration process involves the superposition of a network onto the original cycle. By employing the cycle splitting method, this characteristic can be more intuitively understood during the cycle construction process. Specifically, the S-ORC can be viewed as a combination of a Brayton cycle overlaid onto the basic organic Rankine cycle. In this configuration, the Brayton cycle transfers heat from the cooler not to the environment but to the Rankine cycle through regeneration. This results in a higher thermal efficiency of the system.

(3) The analysis of the effect of the main vapor parameters on the thermal efficiency of different cycles revealed that the supercritical state extraction steam compression regeneration process is well-suited for combined application with turbine exhaust regeneration. This is because the supercritical compression regeneration process aims to increase the average heat absorption temperature, while turbine exhaust regeneration focuses on lowering the average heat release temperature. The combination of these two processes brings the cycle closer to the ideal Carnot cycle. Additionally, when different working fluids are used, the thermal efficiency of the ORC with supercritical extraction and compression regeneration experiences significant improvements. These findings highlight the universality and broad applicability of the supercritical state extraction steam compression regeneration process in ORC applications.

CRediT authorship contribution statement

Enhui Sun: Visualization. **Yueqi Sun:** Methodology. **Shujing Feng:** Investigation. **Lei Zhang:** Data curation. **Jinliang Xu:** Supervision. **Zheng Miao:** Writing – review & editing.

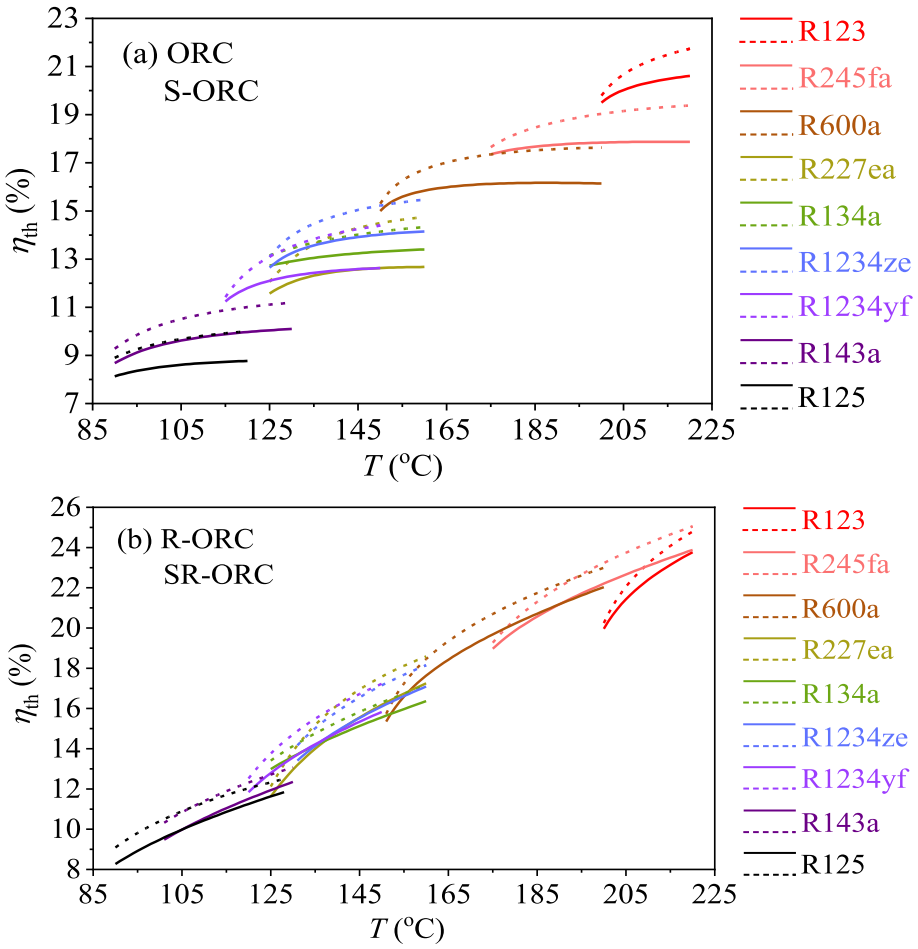

Fig. 12. Cyclic thermal efficiency curves for different working fluids.

Declaration of Competing Interest

The authors declare that they have no known competing financial interests or personal relationships that could have appeared to influence the work reported in this paper.

Data availability

The data that has been used is confidential.

Acknowledgements

The research was supported by the Natural Science Foundation of China (52206010, 52130608, 52076079).

References

[1] Ziviani D, Beyene A, Venturini M. Advances and challenges in ORC systems modeling for low grade thermal energy recovery. Appl Energy 2014;121:79–95.
[2] Rahbar K, Mahmoud S, Al-Dadah RK, Moazami N, Mirhadizadeh SA. Review of organic Rankine cycle for small-scale applications. Energy Convers Manag 2017; 134:135–55.
[3] Mondejar ME, Andreasen JG, Pierobon L, Larsen U, Thern M, Haglind F. A review of the use of organic Rankine cycle power systems for maritime applications. Renew Sustain Energy Rev 2018;91:126–51.
[4] Loni R, Mahian O, Markides CN, Bellos E, le Roux WG, Kasaeian A, et al. A review of solar-driven organic Rankine cycles: Recent challenges and future outlook. Renew Sustain Energy Rev 2021;150:111410.
[5] Gupta PR, Tiwari AK, Said Z. Solar organic Rankine cycle and its poly-generation applications – A review. Sustain Energy Technol Assessments 2022;49:101732.
[6] Ahmadi A, El Haj Assad M, Jamali DH, Kumar R, Li ZX, Salameh T, et al. Applications of geothermal organic Rankine Cycle for electricity production. J Clean Prod 2020;274:122950.
[7] Loni R, Mahian O, Najafi G, Sahin AZ, Rajaee F, Kasaeian A, et al. A critical review of power generation using geothermal-driven organic Rankine cycle. Therm Sci Eng Prog 2021;25:101028.
[8] Sikarwar SS, Surywanshi GD, Patnaikuni VS, Kakunuri M, Vooradi R. Chemical looping combustion integrated Organic Rankine Cycled biomass-fired power plant – Energy and exergy analyses. Renew Energy 2020;155:931–49.
[9] Kavathia K, Prajapati P. A review on biomass-fired CHP system using fruit and vegetable waste with regenerative organic Rankine cycle (RORC). Mater Today: Proc 2020;43:572–8.
[10] Peris B, Navarro-Esbrí J, Mateu-Royo C, Mota-Babiloni A, Molés F, Gutiérrez-Trashorras AJ, et al. Thermo-economic optimization of small-scale Organic Rankine Cycle: A case study for low-grade industrial waste heat recovery. Energy 2020;213:118898.
[11] Loni R, Najafi G, Bellos E, Rajaee F, Said Z, Mazlan M. A review of industrial waste heat recovery system for power generation with Organic Rankine Cycle: Recent challenges and future outlook. J Clean Prod 2021;287:125070.
[12] Tchanche BF, Lambrinos Gr, Frangoudakis A, Papadakis G. Low-grade heat conversion into power using organic Rankine cycles – A review of various applications. Renew Sustain Energy Rev 2011;15(8):3963–79.
[13] Park BS, Usman M, Imran M, Pesyridis A. Review of Organic Rankine Cycle experimental data trends. Energy Convers Manag 2018;173:679–91.
[14] Xu W, Zhao Li, Mao SS, Deng S. Towards novel low temperature thermodynamic cycle: A critical review originated from organic Rankine cycle. Appl Energy 2020; 270:115186.
[15] Schuster A, Karellas S, Aumann R. Efficiency optimization potential in supercritical Organic Rankine Cycles. Energy 2010;35(2):1033–9.
[16] Song C, Gu M, Miao Z, Liu C, Xu J. Effect of fluid dryness and critical temperature on trans-critical organic Rankine cycle. Energy 2019;174:97–109.
[17] Wang M, Zhang J, Liu Q, Tan L. Effects of critical temperature, critical pressure and dryness of working fluids on the performance of the transcritical organic rankine cycle. Energy 2020;202:117663.
[18] Yu C, Xu J, Sun Y. Transcritical pressure Organic Rankine Cycle (ORC) analysis based on the integrated-average temperature difference in evaporators. Appl Therm Eng 2015;88:2–13.
[19] Li J, Liu Q, Ge Z, Duan Y, Yang Z. Thermodynamic performance analyses and optimization of subcritical and transcritical organic Rankine cycles using R1234ze (E) for 100–200 °C heat sources. Energy Convers Manag 2017;149:140–54.

[20] Yağli H, Koç Y, Koç A, Görgülü A, Tandiroğlu A. Parametric optimization and exergetic analysis comparison of subcritical and supercritical organic Rankine cycle (ORC) for biogas fuelled combined heat and power (CHP) engine exhaust gas waste heat. Energy 2016;111:923–32.
[21] Zabek D, Penton J, Reay D. Optimization of waste heat utilization in oil field development employing a transcritical Organic Rankine Cycle (ORC) for electricity generation. Appl Therm Eng 2013;59(1-2):363–9.
[22] Maraver D, Royo J, Lemort V, Quoilin S. Systematic optimization of subcritical and transcritical organic Rankine cycles (ORCs) constrained by technical parameters in multiple applications. Appl Energy 2014;117:11–29.
[23] Javanshir A, Sarunac N, Razzaghpanah Z. Thermodynamic analysis of a regenerative organic Rankine cycle using dry fluids. Appl Therm Eng 2017;123:852–64.
[24] Feng H, Chen W, Chen L, Tang W. Power and efficiency optimizations of an irreversible regenerative organic Rankine cycle. Energy Convers Manag 2020;220:113079.
[25] Sun E, Wang X, Qian Q, Li H, Ma W, Zhang L, et al. Proposal and application of supercritical steam Rankine cycle using supercritical reheating regeneration process and its comparison between S-CO2 Brayton cycle. Energy Convers Manag 2023;280:116798.
[26] Imran M, Usman M, Park BS, Yang Y. Comparative assessment of Organic Rankine Cycle integration for low temperature geothermal heat source applications. Energy 2016;102:473–90.
[27] Feng Y-Q, Wang X, Niaz H, Hung T-C, He Z-X, Jahan Zeb A, et al. Experimental comparison of the performance of basic and regenerative organic Rankine cycles. Energy Convers Manag 2020;223:113459.
[28] Yağlı H, Koç Y, Köse Ö, Koç A, Yumrutaş R. Optimisation of simple and regenerative organic Rankine cycles using jacket water of an internal combustion engine fuelled with biogas produced from agricultural waste. Process Saf Environ Prot 2021;155:17–31.
[29] Le VL, Feidt M, Kheiri A, Pelloux-Prayer S. Performance optimization of low-temperature power generation by supercritical ORCs (organic Rankine cycles) using low GWP (global warming potential) working fluids. Energy 2014;67:513–26.
[30] Braimakis K, Karellas S. Energetic optimization of regenerative Organic Rankine Cycle (ORC) configurations. Energy Convers Manag 2018;159:353–70.
[31] Lemmon EW, Bell IH, Huber ML, McLinden MO. NIST standard reference database 23: reference fluid thermodynamic and transport properties-REFPROP, version 9.0. Gaithersburg: National Institute of Standards and Technology, Standard Reference Data Program; 2010.
[32] Liu J, Xu Y, Zhang Y, Shuai Y, Li B. Multi-objective optimization of low temperature cooling water organic Rankine cycle using dual pinch point temperature difference technologies. Energy 2022;240:122740.
[33] Sun E, Xu J, Li M, Li H, Liu C, Xie J. Synergetics: The cooperative phenomenon in multi-compressions S-CO2 power cycles. Energy Convers Manag X 2020;7:100042.
[34] Xin T, Xu C, Yang Y. A general and simple method for evaluating the performance of the modified steam Rankine cycle: Thermal cycle splitting analytical method. Energy Convers Manag 2020;210:112712.
[35] Liu Q, Shen A, Duan Y. Parametric optimization and performance analyses of geothermal organic Rankine cycles using R600a/R601a mixtures as working fluids. Appl Energy 2015;148:410–20.
[36] Aliahmadi M, Moosavi A, Sadrhosseini H. Multi-objective optimization of regenerative ORC system integrated with thermoelectric generators for low-temperature waste heat recovery. Energy Rep 2021;7:300–13.
[37] Cakici DM, Erdogan A, Colpan CO. Thermodynamic performance assessment of an integrated geothermal powered supercritical regenerative organic Rankine cycle and parabolic trough solar collectors. Energy 2017;120:306–19.
[38] Piñerez GP, Ochoa GV, Duarte-Forero J. Energy, Exergy, And Environmental Assessment Of A Small-Scale Solar Organic Rankine Cycle Using Different Organic Fluids. Heliyon 2021:7.
[39] Mecheri M, Le Moullec Y. Supercritical CO2 Brayton cycles for coal-fired power plants. Energy 2016;103:758–71.
[40] Weiland NT, White CW. Techno-economic analysis of an integrated gasification direct-fired supercritical CO2 power cycle. Fuel 2018;212:613–25.
[41] Vetter C, Wiemer H-J, Kuhn D. Comparison of sub- and supercritical Organic Rankine Cycles for power generation from low-temperature/low-enthalpy geothermal wells, considering specific net power output and efficiency. Appl Therm Eng 2013;51(1-2):871–9.
[42] Liu X, Niu J, Wang J, Su L, Dong L. Thermodynamic performance of subcritical double-pressure organic Rankine cycles driven by geothermal energy. Appl Therm Eng 2021;195:117162.
[43] Xu J, Zheng Y, Wang Y, Yang X, Yu C, Xie X, et al. An actual thermal efficiency expression for heat engines: Effect of heat transfer roadmaps. Int J Heat Mass Transf 2017;113:556–68.
[44] Zinsalo JM, Lamarche L, Raymond J. Performance analysis and working fluid selection of an Organic Rankine Cycle Power Plant coupled to an Enhanced Geothermal System. Energy 2022;245:123259.
[45] Lettieri C, Yang D, Spakovszky Z. An investigation of condensation effects in supercritical carbon dioxide compressors. J Eng Gas Turbines Power 2015;137:082602.
[46] Poerner M, Musgrove G, Beck G. Liquid CO_2 formation, impact, and mitigation at the inlet to a supercritical CO_2 compressor. Proc ASME Turbo Expo 2016.